

Synthesis and Protonation of [RuH(NBD)(2,6-(Ph₂PCH₂)₂C₆H₃)]

Sheng Hua Liu,[†] Sze Ming Ng,[†] Ting Bin Wen,[†] Zhong Yuan Zhou,[‡]
Zhenyang Lin,^{*,†} Chak Po Lau,^{*,†} and Guochen Jia^{*,†}

Department of Chemistry, The Hong Kong University of Science and Technology,
Clear Water Bay, Kowloon, Hong Kong, and Department of Applied Biology & Chemical
Technology, The Hong Kong Polytechnic University, Hung Hom, Kowloon, Hong Kong

Received July 2, 2002

Treatment of [RuCl(PPh₃)(PCP)] (PCP = 2,6-(Ph₂PCH₂)₂C₆H₃) with norbornadiene (NBD) in the presence of CuCl produces [RuCl(NBD)(PCP)]. Reaction of [RuCl(NBD)(PCP)] with TlOTf gives [Ru(OTf)(NBD)(PCP)], which reacts with NaBH₄ to produce [RuH(NBD)(PCP)]. Protonation of [RuH(NBD)(PCP)] with acetic acid in the presence of PPh₃ gives norbornene and [Ru(OAc)(PPh₃)(PCP)]. Protonation of [RuH(NBD)(PCP)] with HOTf gives norbornane and [Ru(OTf)(NBD)(PCP)]. Protonation of [RuH(NBD)(PCP)] with HOTf in the presence of MeCN gives norbornene, [Ru(MeCN)(NBD)(PCP)]OTf, and [Ru(MeCN)₃(PCP)]OTf. In the protonation reactions, the NBD is likely hydrogenated through the dihydrogen intermediate [Ru(H₂)(NBD)(PCP)]⁺. A computational study shows that hydrogen transfer from the dihydrogen to the NBD ligand of [Ru(H₂)(NBD)(PCP)]⁺ proceeds through a stepwise mechanism.

Introduction

Studies on the reactivity of coordinated dihydrogen toward organic ligands (e.g. alkyls, vinyls, acetylides, vinylidenes, olefins) are of fundamental importance, because such investigations may help to understand the mechanisms of reactions involving dihydrogen complexes^{1,2} and to develop new chemistry and catalytic reactions based on σ -complexes. In the past decade, significant progress has been made in this direction. It has been demonstrated with well-defined dihydrogen complexes that complexes of the type [M(R)(H₂)L_n] can undergo intramolecular hydrogen transfer from the coordinated dihydrogen ligand to the α -carbon of R

groups such as alkyls, vinyls,³ and acetylides⁴ to form [MHL_n] and RH. These reactions have also been proposed or inferred as the key steps in the catalytic hydrogenation of olefins and acetylenes.^{5–8} Hydrogen transfer from a coordinated dihydrogen ligand to the β -carbons of vinylidene ligands has been proposed for the reactions of [OsCl₂H₂(P(*i*-Pr)₃)₂] with HC≡CR to give the carbyne complexes [OsCl₂H(≡CCH₂R)(P(*i*-Pr)₃)₂] via the intermediates [OsCl₂(H₂)(=C=CCHR)(P(*i*-Pr)₃)₂].⁹

This work is related to the reactivity of coordinated dihydrogen toward olefin ligands. Olefin–dihydrogen complexes have been suggested as intermediates in several catalytic reactions.^{8,10–11} For example, the dihydrogen complexes [M(H₂)(η^4 -NBD)(CO)₃] (M = Cr, Mo, W) have been proposed as the intermediates for

[†] The Hong Kong University of Science and Technology.

[‡] The Hong Kong Polytechnic University.

(1) (a) Crabtree, R. H. *Angew. Chem., Int. Ed. Engl.* **1993**, *32*, 789. (b) Heinekey, D. M.; Oldham, W. J., Jr. *Chem. Rev.* **1993**, *93*, 913. (c) Jessop, P. G.; Morris, R. H. *Coord. Chem. Rev.* **1992**, *121*, 155. (d) Esteruelas, M. A.; Oro, L. A. *Chem. Rev.* **1998**, *98*, 577. (e) Kubas, G. J. *Dihydrogen and σ -Bond Complexes*; Kluwer Academic/Plenum Press: New York, 2001. (f) Peruzzini, M.; Poli, R. *Recent Advances in Hydride Chemistry*; Elsevier: Amsterdam, The Netherlands, 2001.

(2) For recent work on dihydrogen complexes, see for example: (a) Law, J. K.; Mellows, H.; Heinekey, D. M. *J. Am. Chem. Soc.* **2002**, *124*, 1024. (b) Cameron, T. M.; Ortiz, C. G.; Ghiviriga, I.; Abboud, K. A.; Boncella, J. M. *J. Am. Chem. Soc.* **2002**, *124*, 922. (c) Heinekey, D. M.; Law, J. K.; Schultz, S. M. *J. Am. Chem. Soc.* **2001**, *123*, 12728. (d) Fan, H. J.; Hall, M. B. *J. Am. Chem. Soc.* **2001**, *123*, 3828. (e) Law, J. K.; Mellows, H.; Heinekey, D. M. *J. Am. Chem. Soc.* **2001**, *123*, 2085. (f) Abdur-Rashid, K.; Fong, T. P.; Greaves, B.; Gusev, D. G.; Hinman, J. G.; Landau, S. E.; Lough, A. J.; Morris, R. H. *J. Am. Chem. Soc.* **2000**, *122*, 9155. (g) Toner, A. J.; Grundermann, S.; Clot, E.; Limbach, H. H.; Donnadiet, B.; Sabo-Etienne, S.; Chaudret, B. *J. Am. Chem. Soc.* **2000**, *122*, 6777. (h) Li, S.; Hall, M. B.; Eckert, J.; Jensen, C. M.; Albinati, A. *J. Am. Chem. Soc.* **2000**, *122*, 2903. (i) Kaulen, C.; Pala, C.; Hu, C.; Ganter, C. *Organometallics* **2001**, *20*, 1614. (j) Mathew, N.; Jagirdar, B. R.; Gopalan, R. S.; Kulkarni, G. U. *Organometallics* **2000**, *19*, 4506. (k) Hung, M. Y.; Ng, S. M.; Zhou, Z.; Lau, C. P.; Jia, G. *Organometallics* **2000**, *19*, 3692. (l) Rodriguez, V.; Atheaux, I.; Donnadiet, B.; Sabo-Etienne, S.; Chaudret, B. *Organometallics* **2000**, *19*, 2916. (m) Bianchini, C.; Barbaro, P.; Scapacci, G.; Zanobini, F. *Organometallics* **2000**, *19*, 2450. (n) Abdur-Rashid, K.; Gusev, D. G.; Lough, A. J.; Morris, R. H. *Organometallics* **2000**, *19*, 1652.

(3) Liu, S. H.; Lo, S. T.; Wen, T. B.; Zhou, Z. Y.; Lau, C. P.; Jia, G. *Organometallics* **2001**, *20*, 667.

(4) (a) Tenorio, M. J.; Puerta, M. C.; Valerga, P. *J. Chem. Soc., Chem. Commun.* **1993**, 1750. (b) Espuelas, J.; Esteruelas, M. A.; Lahoz, F. J.; Oro, L. A.; Valero, C. *Organometallics* **1993**, *12*, 663.

(5) (a) Bianchini, C.; Meli, A.; Peruzzini, M.; Frediani, P.; Bohanna, C.; Esteruelas, M. A.; Oro, L. A. *Organometallics* **1992**, *11*, 138. (b) Bianchini, C.; Bohanna, C.; Esteruelas, M. A.; Frediani, P.; Meli, A.; Oro, L. A.; Peruzzini, M. *Organometallics* **1992**, *11*, 3837.

(6) (a) Andriollo, A.; Esteruelas, M. A.; Meyer, U.; Oro, L. A.; Sánchez-Delgado, R. A.; Sola, E.; Valero, C.; Werner, H. *J. Am. Chem. Soc.* **1989**, *111*, 7431. (b) Esteruelas, M. A.; Oro, L. A.; Valero, C. *Organometallics* **1992**, *11*, 3362.

(7) Crabtree, R. H. *The Organometallic Chemistry of the Transition Metals*, 3rd ed.; Wiley: New York, 2001; pp 237–238.

(8) Chan, W. C.; Lau, C. P.; Chen, Y. Z.; Fang, Y. Q.; Ng, S. M.; Jia, G. *Organometallics* **1997**, *16*, 34.

(9) Espuelas, J.; Esteruelas, M. A.; Lahoz, F. J.; Oro, L. A.; Ruiz, N. *J. Am. Chem. Soc.* **1993**, *115*, 4683.

(10) (a) Jackson, S. A.; Hodges, P. M.; Poliakov, M.; Turner, J. J.; Grevels, F. W. *J. Am. Chem. Soc.* **1990**, *112*, 1221. (b) Hodges, P. M.; Jackson, S. A.; Jacke, J.; Poliakov, M.; Turner, J. J.; Grevels, F. W. *J. Am. Chem. Soc.* **1990**, *112*, 1234. (c) Thomas, A.; Haake, M.; Grevels, F. W.; Bargon, J. *Angew. Chem., Int. Ed. Engl.* **1994**, *33*, 755. (d) Childs, G. I.; Cooper, A. I.; Nolan, T. F.; Carrott, M. J.; George, M. W.; Poliakov, M. *J. Am. Chem. Soc.* **2001**, *123*, 6857.

(11) Budzelaar, P. H. M.; Moonen, N. N. P.; de Gelder, R.; Smits, J. M. M.; Gal, A. W. *Eur. J. Inorg. Chem.* **2000**, 753.

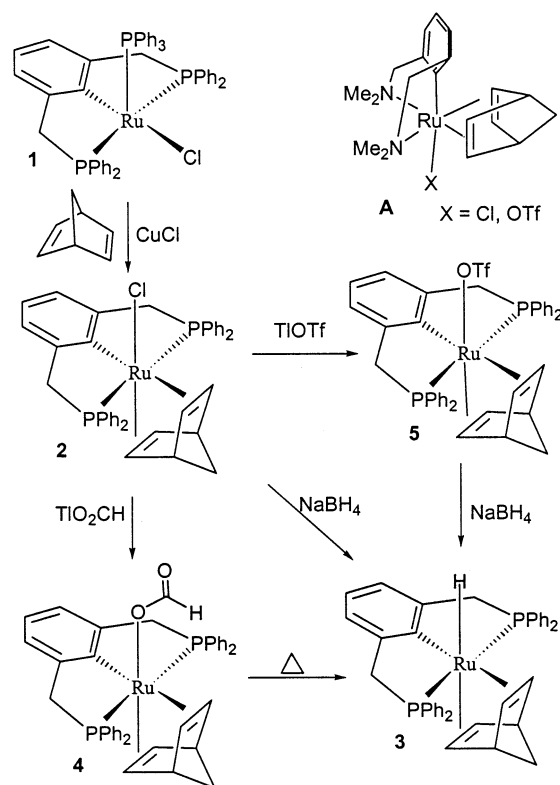
photocatalytic hydrogenation of norbornadiene using $[M(CO)_6]$;¹⁰ the complexes $[Rh\{(2,6-C_6H_3Me_2)NCMeCHCMeN(2,6-C_6H_3Me_2)\}(H_2)(olefin)]$ were proposed as the intermediates for catalytic hydrogenation of olefins using $[Rh\{(2,6-C_6H_3Me_2)NCMeCHCMeN(2,6-C_6H_3Me_2)\}(COE)]$,¹¹ and the complexes $[Ru(Tp)(PPh_3)(H_2)(olefin)]^+$ were thought to be involved in catalytic hydrogenation of olefins using $[Ru(Tp)(PPh_3)_x(CH_3CN)_{3-x}]^+$ ($x = 1, 2$).⁸ A few olefin–dihydrogen complexes have been characterized by IR¹⁰ and NMR^{11,12} spectroscopy. To model reactions involving olefin–dihydrogen complexes, it is obviously desirable to demonstrate stoichiometric intramolecular hydrogen transfer (from dihydrogen to olefin ligands) reactions of olefin–dihydrogen complexes. However, very little work has been previously done in this regard. In our approach to model stoichiometric hydrogen transfer from H_2 to olefin ligands, we have studied protonation reactions of $[MH(olefin)L_n]$,¹² hoping that the protonation reactions may give $[M(H_2)(olefin)L_n]^+$ or hydrogen-transferred products. In our previous study, we have shown that protonation of $[Ru(Cp^*)H(NBD)]$, where H is cis to both of the double bonds of NBD, produces the hydrogenated product nortricyclene.^{12a} In this work, the protonation reactions of $[RuH(NBD)(PCP)]$ (PCP = 2,6-(Ph₂PCH₂)₂C₆H₃) were investigated. $[RuH(NBD)(PCP)]$ is different from $[Ru(Cp^*)H(NBD)]$ in that the hydride is only cis to one of the double bonds of NBD. Thus, this provides us an opportunity to see how the position of the hydride relative to the double bonds of NBD may affect the reactivity. In a related study, Esteruelas et al. have investigated the protonation reactions of $[OsH_2(diolefin)(P(i-Pr)_3)_2]$ (diolefin = NBD, cyclohexadiene).¹³

In hydrogenation involving the olefin–dihydrogen complexes $[M(H_2)(olefin)L_n]$, hydrogen transfer from the coordinated H_2 ligand to the olefin ligands could go through a concerted mechanism or through a stepwise mechanism in which one of the hydrogens from the coordinated H_2 is first transferred to the olefin ligands to give the hydrido alkyl complexes $[MH(alkyl)L_n]$ followed by reductive elimination. However, detailed pathways for the hydrogen transfer process have rarely been addressed previously. In this work, we have studied the reaction pathways for the conversion of $[Ru(H_2)(NBD)(PCP)]^+$ to $[Ru(NBE)(PCP)]^+$ (NBE = norbornene) by computational chemistry, to see if the hydrogen transfer process is stepwise or concerted.

Results and Discussion

Synthesis of $[RuH(NBD)(PCP)]$. As mentioned previously, we intend to model stoichiometric intramolecular hydrogen transfer from coordinated dihydrogen to olefin ligands. It is known that protonation of $[RuH_2L_4]$ (L = phosphine, phosphite) can produce the dihydrogen complexes $[RuH(H_2)L_4]^+$.¹⁴ Thus, we prepared the hydride complex $[RuH(NBD)(PCP)]$, expecting that subsequent protonation of the hydride complex would produce the dihydrogen complex $[Ru(H_2)(NBD)(PCP)]^+$ or hydrogen-transferred products. The biden-

Scheme 1



tate olefin NBD and the tridentate PCP ligand have been used in the study, because such a system may give complexes with well-defined geometry. A number of ruthenium^{15–18} and osmium¹⁹ complexes with PCP or PCP-related ligands have been reported recently. In these complexes, the PCP ligand is usually coordinated to the metal centers in a meridional fashion.

The synthetic route to the hydride complex $[RuH(NBD)(PCP)]$ (**3**) is outlined in Scheme 1. Treatment of $[RuCl(PPh_3)(PCP)]$ (**1**) with NBD in the presence of

(14) See for example: (a) Schlaf, M.; Lough, A. J.; Morris, R. H. *Organometallics* **1997**, *16*, 1253. (b) Bianchini, C.; Masi, D.; Peruzzini, M.; Casarin, M.; Maccato, C.; Rizzi, G. A. *Inorg. Chem.* **1997**, *36*, 1061. (c) Ayllón, J. A.; Gervaux, C.; Sabo-Etienne, S.; Chaudret, B. *Organometallics* **1997**, *16*, 2000. (d) Rocchini, E.; Mezzetti, A.; Rüegger, H.; Burckhardt, U.; Gramlich, V.; Del Zotto, A.; Martinuzzi, P.; Rigo, P. *Inorg. Chem.* **1997**, *36*, 711. (e) Gusev, D. G.; Hübener, R.; Orama, O.; Berke, H. *J. Am. Chem. Soc.* **1997**, *117*, 3716 and references therein. (f) Cappellani, E. P.; Drouin, S. D.; Jia, G.; Maltby, P. A.; Morris, R. H.; Schweitzer, C. T. *J. Am. Chem. Soc.* **1994**, *116*, 3375.

(15) (a) Dijkstra, H. P.; Albrecht, M.; van Koten, G. *Chem. Commun.* **2002**, 126. (b) Albrecht, M.; van Koten, G. *Angew. Chem., Int. Ed.* **2001**, *40*, 3750. (c) Dani, P.; Richter, B.; van Klink, G. P. M.; van Koten, G. *Eur. J. Inorg. Chem.* **2001**, 125. (d) Dani, P.; Toorneman, M. A. M.; van Klink, G. P. M.; van Koten, G. *Organometallics* **2000**, *19*, 5287. (e) Dani, P.; Albrecht, M.; van Klink, G. P. M.; van Koten, G. *Organometallics* **2000**, *19*, 4468. (f) Dani, P.; Karlen, T.; Gossage, R. A.; Gladiali, S.; van Koten, G. *Angew. Chem., Int. Ed.* **2000**, *39*, 743. (g) Karlen, T.; Dani, P.; Grove, D. M.; Steenwinkel, P.; van Koten, G. *Organometallics* **1996**, *15*, 5687.

(16) (a) Gusev, D. G.; Dolgushin, F. M.; Antipin, M. Y. *Organometallics* **2000**, *19*, 3429. (b) Gusev, D. G.; Madott, M.; Dolgushin, F. M.; Lyssenko, K. A.; Antipin, M. Y. *Organometallics* **2000**, *19*, 1734.

(17) van der Boom, M. E.; Kraatz, H. B.; Hassner, L.; Ben-David, Y.; Milstein, D. *Organometallics* **1999**, *18*, 3873.

(18) (a) Jia, G.; Lee, H. M.; Xia, H. P.; Williams, I. D. *Organometallics* **1996**, *15*, 5453. (b) Jia, G.; Lee, H. M.; Williams, I. D. *J. Organomet. Chem.* **1997**, *534*, 173. (c) Lee, H. M.; Yao, J. Z.; Jia, G. *Organometallics* **1997**, *16*, 3927.

(19) (a) Wen, T. B.; Cheung, Y. K.; Yao, J.; Wong, W. T.; Zhou, Z. Y.; Jia, G. *Organometallics* **2000**, *19*, 3803. (b) Gusev, D. G.; Dolgushin, F. M.; Antipin, M. Y. *Organometallics* **2001**, *20*, 1001. (c) Gauvin, R. M.; Rozenberg, H.; Shimon, L. J. W.; Milstein, D. *Organometallics* **2001**, *20*, 1719.

(12) (a) Jia, G.; Ng, W. S.; Lau, C. P. *Organometallics* **1998**, *17*, 4538. (b) Liu, S. H.; Yang, S. Y.; Lo, S. T.; Xu, Z.; Ng, W. S.; Wen, T. B.; Zhou, Z. Y.; Lin, Z.; Lau, C. P.; Jia, G. *Organometallics* **2001**, *20*, 4161.

(13) Castillo, A.; Esteruelas, M. A.; Oñate, E.; Ruiz, N. *J. Am. Chem. Soc.* **1997**, *119*, 9691.

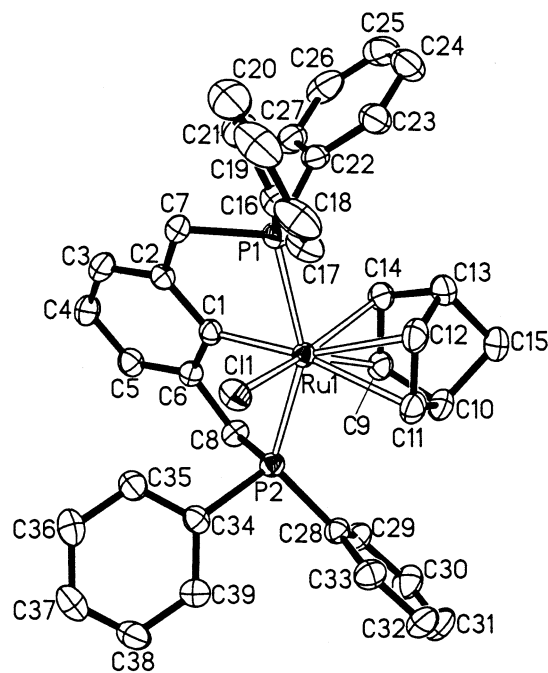


Figure 1. Molecular structure of [RuCl(NBD)(PCP)]. Hydrogen atoms are omitted for clarity.

excess CuCl produced the chloro complex [RuCl(NBD)(PCP)] (**2**), which was isolated as a yellow solid in ca. 80% yield. No reaction was observed between **1** and NBD if CuCl was not used. Cuprous chloride has been shown to be a good phosphine scavenger.²⁰ A recent example of using CuCl as the scavenger of phosphines was reported by Grubbs et al. in the isolation of [Ru(O-*t*-Bu)₂(=CHPh)(PCy₃)] from the reaction of [RuCl₂(=CHPh)(PCy₃)₂] with KO-*t*-Bu.^{20b}

The structure of **2** has been confirmed by an X-ray diffraction study. The molecular structure of **2** is depicted in Figure 1. The crystallographic details and selected bond distances and angles are given in Tables 1 and 2, respectively. The structure of **2** can be described as a distorted octahedron in which two vertexes are occupied by the two double bonds of NBD and three vertexes are occupied by a meridionally coordinated PCP ligand. One of the double bonds of NBD is trans to the chloride, while the other one is trans to the ipso carbon of the PCP ligand. The bond distances between ruthenium and the carbons of the double bond trans to the chloride are slightly shorter than those between ruthenium and the carbons of the double bond trans to the aryl ligand, reflecting the stronger trans influence of the aryl ligand. The Ru-C(olefin) bond distances are similar to those of reported Ru(η^4 -NBD) complexes such as [RuCl₂(NBD)(PPh₃)₂],²¹ [Ru(η^5 -C₉H₇)Cl(NBD)],²² [Ru(Cp*)(NBD)(H₂O)]BF₄,²³ and [RuX(NBD)(2,6-(Me₂NCH₂)₂-C₆H₃)] (X = Cl, OTf).²⁴ The structural feature associated with the Ru(PCP) fragment is normal compared

Table 1. Crystal Data and Structure Refinement Details for the Complexes [RuCl(NBD)(PCP)] (2**), [Ru(OAc)(PPh₃)(PCP)] (**6**), and [Ru(MeCN)(NBD)(PCP)]OTf (**7**)**

	2	6	7
formula	C ₃₉ H ₃₅ ClP ₂ Ru	C ₅₂ H ₄₅ O ₂ P ₃ Ru	C ₄₂ H ₃₈ F ₃ NO ₃ P ₂ RuS
fw	702.13	895.86	856.80
cryst syst	orthorhombic	triclinic	monoclinic
space group	<i>P</i> 2 ₁ 2 ₁ 2 ₁ (No. 19) ^a	<i>P</i> 1 (No. 2)	<i>P</i> 2 ₁ / <i>c</i> (No. 14)
<i>a</i> , Å	11.923(2)	10.6517(16)	15.318(3)
<i>b</i> , Å	13.351(3)	11.0510(16)	14.450(2)
<i>c</i> , Å	20.299(4)	19.997(3)	17.763(3)
α , deg	90	89.891(3)	90
β , deg	90	78.283(3)	104.142(3)
γ , deg	90	71.252(3)	90
<i>V</i> , Å ³	3231.3(11)	2177.5(6)	3812.8(10)
<i>Z</i>	4	2	4
<i>d</i> _{calcd} , g cm ⁻³	1.443	1.366	1.493
cryst dimens, mm	0.30 × 0.22 × 0.20	0.28 × 0.24 × 0.12	0.35 × 0.35 × 0.12
θ range, deg	2.29–27.55	1.95–27.52	1.37–25.74
abs coeff, cm ⁻¹	6.94	5.11	6.05
no. of rflns collected	22 043	14 787	25 335
no. of indep rflns	7449 (<i>R</i> _{int} = 0.0267)	9874 (<i>R</i> _{int} = 0.0185)	8758 (<i>R</i> _{int} = 0.0342)
no. of obsd rflns (<i>I</i> > 2 σ (<i>I</i>))	6717	7955	5834
no. of params refined	388	523	478
goodness of fit on <i>F</i> ²	1.008	0.971	1.042
<i>R</i> 1 (<i>I</i> > 2 σ (<i>I</i>))	0.0261	0.0319	0.0474
<i>wR</i> 2 (<i>I</i> > 2 σ (<i>I</i>))	0.0576	0.0743	0.1384
largest diff peak, e Å ⁻³	0.680	0.600	1.391
largest diff hole, e Å ⁻³	-0.274	-0.328	-0.817

^a Absolute structure parameter: -0.033(18).

Table 2. Selected Bond Lengths (Å) and Bond Angles (deg) for [RuCl(NBD)(PCP)] (2**)**

Ru(1)–P(1)	2.3816(7)	Ru(1)–P(2)	2.3632(7)
Ru(1)–Cl(1)	2.4309(7)	Ru(1)–C(1)	2.120(2)
Ru(1)–C(9)	2.210(2)	Ru(1)–C(11)	2.286(2)
Ru(1)–C(12)	2.285(3)	Ru(1)–C(14)	2.189(2)
C(9)–C(14)	1.392(3)	C(11)–C(12)	1.370(4)
C(9)–C(10)	1.545(4)	C(10)–C(11)	1.539(4)
C(12)–C(13)	1.545(4)	C(13)–C(14)	1.530(4)
C(10)–C(15)	1.544(4)	C(13)–C(15)	1.546(4)
P(1)–Ru(1)–P(2)	152.49(2)	P(1)–Ru(1)–Cl(1)	81.45(2)
P(2)–Ru(1)–Cl(1)	87.91(2)	C(1)–Ru(1)–Cl(1)	93.81(7)
C(1)–Ru(1)–P(1)	79.75(6)	C(1)–Ru(1)–P(2)	75.71(6)
C(1)–Ru(1)–C(9)	101.44(9)	C(1)–Ru(1)–C(14)	100.80(10)
C(1)–Ru(1)–C(11)	160.23(9)	C(1)–Ru(1)–C(12)	158.98(9)
C(9)–Ru(1)–P(1)	119.93(6)	C(14)–Ru(1)–P(1)	83.34(7)
C(11)–Ru(1)–P(1)	118.46(7)	C(12)–Ru(1)–P(1)	83.93(7)
C(9)–Ru(1)–P(2)	77.53(7)	C(14)–Ru(1)–P(2)	113.20(7)
C(11)–Ru(1)–P(2)	87.80(7)	C(12)–Ru(1)–P(2)	122.68(7)
C(9)–Ru(1)–Cl(1)	155.46(6)	C(14)–Ru(1)–Cl(1)	156.65(7)
C(11)–Ru(1)–Cl(1)	96.43(7)	C(12)–Ru(1)–Cl(1)	96.79(8)
C(14)–Ru(1)–C(9)	36.89(9)	C(12)–Ru(1)–C(11)	34.88(10)
C(9)–Ru(1)–C(11)	63.75(10)	C(14)–Ru(1)–C(12)	63.96(11)
C(9)–Ru(1)–C(12)	75.43(10)	C(14)–Ru(1)–C(11)	75.51(10)

to those of other structurally characterized Ru(PCP) complexes such as [RuCl(PPh₃)(PCP)]^{18b} and [Ru(PCP)(PCHP)]OTf.^{15d}

Consistent with the solid-state structure, the ³¹P{¹H} NMR spectrum of **2** in C₆D₆ showed a singlet at 55.4 ppm. The ¹H NMR spectrum in C₆D₆ showed five NBD signals: the olefinic protons displayed two signals at

(20) (a) Dias, E. L.; Nguyen, S. T.; Grubbs, R. H. *J. Am. Chem. Soc.* **1997**, *119*, 3887. (b) Sanford, M. S.; Henling, L. M.; Day, M. W.; Grubbs, R. H. *Angew. Chem., Int. Ed.* **2000**, *39*, 3451. (c) Wakamatsu, H.; Blechert, S. *Angew. Chem., Int. Ed.* **2002**, *41*, 794.

(21) Bergbreiter, D. E.; Bursten, B. E.; Bursten, M. S.; Cotton, F. A. *J. Organomet. Chem.* **1981**, *205*, 407.

(22) Álvarez, P.; Gimeno, J.; Lastra, E.; García-Granda, S.; Van der Maelen, J. F.; Bassetti, M. *Organometallics* **2001**, *20*, 3762.

(23) Suzuki, H.; Kakigano, T.; Fukui, H.; Tanaka, M.; Moro-oka, Y. *J. Organomet. Chem.* **1994**, *473*, 295.

(24) Sutter, J. P.; James, S. L.; Steenwinkel, P.; Karlen, T.; Grove, D. M.; Veldman, N.; Smeets, W. J. J.; Spek, A. L.; van Koten, G. *Organometallics* **1996**, *15*, 941.

2.90 and 4.94 ppm, the bridgehead protons displayed only one signal at 2.70 ppm, and the methylene protons displayed two signals at 0.65 and 0.88 ppm. The ^1H NMR data of NBD are in agreement with the structure in which the two methylene protons of NBD are non-equivalent but the two bridgehead protons of NBD are equivalent.

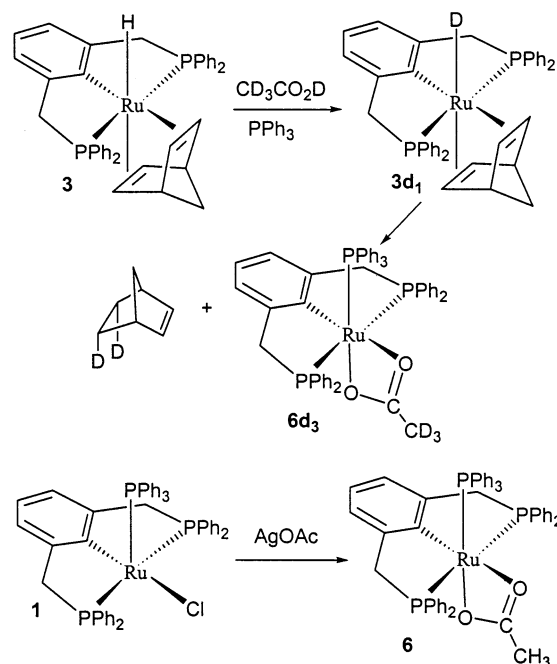
Reported compounds closely related to **2** are $[\text{RuX}(\text{NBD})(2,6\text{-}(\text{Me}_2\text{NCH}_2)_2\text{C}_6\text{H}_3)]$ ($\text{X} = \text{Cl}, \text{OTf}$; see structure **A** shown in Scheme 1 for their geometry), which were reported recently by van Koten et al.²⁴ Unlike complex **2**, the tridentate $2,6\text{-}(\text{Me}_2\text{NCH}_2)_2\text{C}_6\text{H}_3$ ligand in **A** adopts a pseudofacial coordination mode and the double bonds of NBD are trans to the nitrogen atoms of the aryldiamine ligand.

To convert **2** to the hydride complex $[\text{RuH}(\text{NBD})(\text{PCP})]$ (**3**), we have treated complex **2** with NaBH_4 . The reaction in THF is very sluggish, and no reaction was observed between **2** and NaBH_4 at room temperature. The expected hydride **3** along with some uncharacterized phosphorus-containing species were produced when a mixture of **2** and NaBH_4 was refluxed in THF for 8 h. Apparently, the chloride is bound to the ruthenium very tightly so that the metathesis reaction could not occur easily. In an alternative approach to prepare hydride complex **3**, we have treated complex **2** with TiO_2CH , hoping that complex **3** may be obtained via the formate intermediate $[\text{Ru}(\text{O}_2\text{CH})(\text{NBD})(\text{PCP})]$. Formation of $[\text{MHL}_n]$ by elimination of CO_2 from formate complexes $[\text{M}(\text{O}_2\text{CH})\text{L}_n]$ are known reactions.²⁵ As expected, reaction of **2** with TiO_2CH in THF produced the formate complex $[\text{Ru}(\text{O}_2\text{CH})(\text{NBD})(\text{PCP})]$ (**4**). The presence of the formate ligand in complex **4** is indicated by the ^1H NMR spectrum, which showed the signal of O_2CH at 7.97 ppm (in C_6D_6). The formate complex **4** presumably has a coordination sphere similar to that of **2**, as judged on the basis of the NMR data. The hydride complex **3** was produced when the formate complex **4** was refluxed in benzene for 16 h. However, the reaction is not clean and small amounts of uncharacterized compounds were also produced under the reaction conditions.

It was found that the hydride complex **3** could be easily prepared from the reactions of NaBH_4 with $[\text{Ru}(\text{OTf})(\text{NBD})(\text{PCP})]$ (**5**), which was in turn prepared by treating **2** with TiOTf . Complex **5** has ^1H and $^{31}\text{P}\{^1\text{H}\}$ NMR data very similar to those of complex **2**, indicating that they have similar coordination spheres. The hydride complex **3** has been characterized by NMR spectroscopy and elemental analysis. Its structure can be readily assigned on the basis of the NMR data. The ^1H NMR spectrum in CD_2Cl_2 showed the hydride signal as a triplet at -11.53 ppm with a $^2J(\text{PH})$ value of 22.5 Hz. Thus, the hydride is cis to the two PPh_2 groups. In the $^{31}\text{C}\{^1\text{H}\}$ NMR spectrum, the methylene carbons of PCP exhibit a virtual triplet at 47.2 ppm, suggesting that the PCP is meridionally coordinated to ruthenium.^{18c} The ^{13}C NMR data of NBD of **3** indicate that the two double bonds are nonequivalent but the two bridgehead CH's are equivalent. Thus, **3** must have a structure similar to that of **2**. In agreement with the structure,

(25) See for example: (a) Ogo, S.; Makihara, N.; Kaneko, Y.; Watanabe, Y. *Organometallics* **2001**, *20*, 4903. (b) Lo, H. C.; Leiva, C.; Buriez, O.; Kerr, J. B.; Olmstead, M. M.; Fish, R. H. *Inorg. Chem.* **2001**, *40*, 6705. (c) Jia, G.; Meek, D. W.; Gallucci, J. C. *Inorg. Chem.* **1991**, *30*, 403.

Scheme 2



the $^{31}\text{P}\{^1\text{H}\}$ NMR spectrum in CD_2Cl_2 exhibited a singlet at 76.9 ppm. Reported hydride complexes with a NBD ligand related to **3** include $[\text{MClH}(\text{NBD})(\text{PPh}_3)_2]$ ($\text{M} = \text{Ru},^{26} \text{Os}^{27}$), $[\text{M}(\text{OTf})\text{H}(\text{NBD})(\text{PPh}_3)_2]$ ($\text{M} = \text{Ru}, \text{Os}$),²⁷ $[\text{Ru}(\text{Cp}^*)\text{H}(\text{NBD})]$,^{12a} and $[\text{OsH}_2(\text{NBD})(\text{P}(i\text{-Pr})_3)_2]$.¹³

Protonation of $[\text{RuH}(\text{NBD})(\text{PCP})]$ with Acetic Acid. Protonation of hydride complexes is one of the most common pathways to prepare dihydrogen complexes.¹ It is also known that protonation of the olefin-hydride complexes $[\text{MH}(\text{olefin})\text{L}_n]$ could give either dihydrogen complexes or dihydride complexes, depending on the electron richness of the metal centers. For example, protonation of $[\text{Ru}(\text{Cp}^*)\text{H}(\text{COD})]$ produces $[\text{Ru}(\text{Cp}^*)(\text{H}_2)(\text{COD})]^+$,^{12a} protonation of the more electron-rich complex $[\text{OsH}_2(\text{NBD})(\text{P}(i\text{-Pr})_3)_2]$ produces the trihydride complex $[\text{OsH}_3(\text{NBD})(\text{P}(i\text{-Pr})_3)_2]^+$.¹³ Since $[\text{RuH}(\text{H}_2)(\text{dppe})_2]^+$ contains a dihydrogen ligand^{14f} and NBD is less electron-donating than dppe, it is reasonable to expect that protonation of **3** will generate the dihydrogen complex $[\text{Ru}(\text{H}_2)(\text{NBD})(\text{PCP})]^+$, which may undergo hydrogen transfer reactions to give norbornene and the metal fragment $[\text{Ru}(\text{PCP})]^+$. To obtain easily characterizable metal complexes, the protonation was performed with acetic acid in the presence of PPh_3 , in the hope that the metal fragment $[\text{Ru}(\text{PCP})]^+$, if produced, will combine with acetate and/or PPh_3 to give well-defined stable complexes. A control experiment shows that **3** is unreactive toward PPh_3 . In the presence of PPh_3 , complex **3** slowly reacted with excess $\text{CD}_3\text{CO}_2\text{D}$ to give $[\text{Ru}(\text{O}_2\text{CCD}_3)(\text{PPh}_3)(\text{PCP})]$ (**6d3**) and partially deuterated norbornene (see Scheme 2). The norbornene generated can be readily identified by ^2H and ^1H NMR spectra. The ^2H NMR spectrum of the NBE generated in the reaction shows a ^2H signal at 0.97 ppm, indicating that the deuterium is only incorporated at the endo position of NBE.²⁸ The results also indicate that the

(26) Hallman, P. S.; McGarvey, B. R.; Wilkinson, G. *J. Chem. Soc. A* **1968**, 3143.

(27) Lo, S. T.; Xu, Z.; Wen, T. B.; Ng, W. S.; Liu, S. H.; Zhou, Z. Y.; Lin, Z.; Lau, C. P.; Jia, G. *Organometallics* **2000**, *19*, 4523.

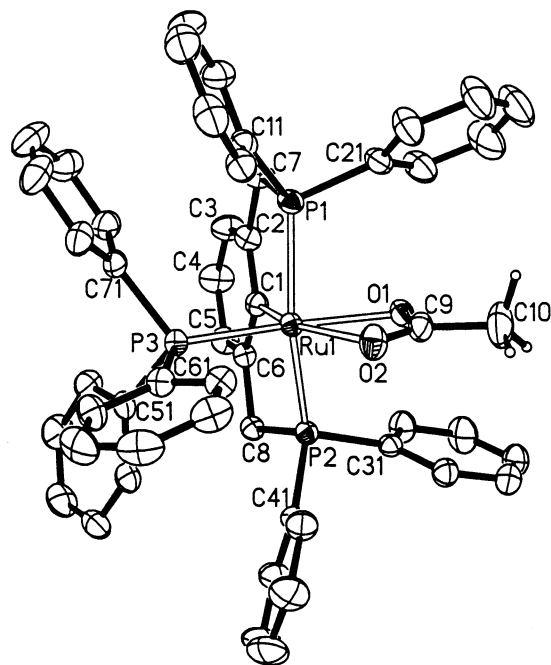


Figure 2. Molecular structure of [Ru(OAc)(PPh₃)(PCP)]. Hydrogen atoms of PPh₃ and PCP are omitted for clarity.

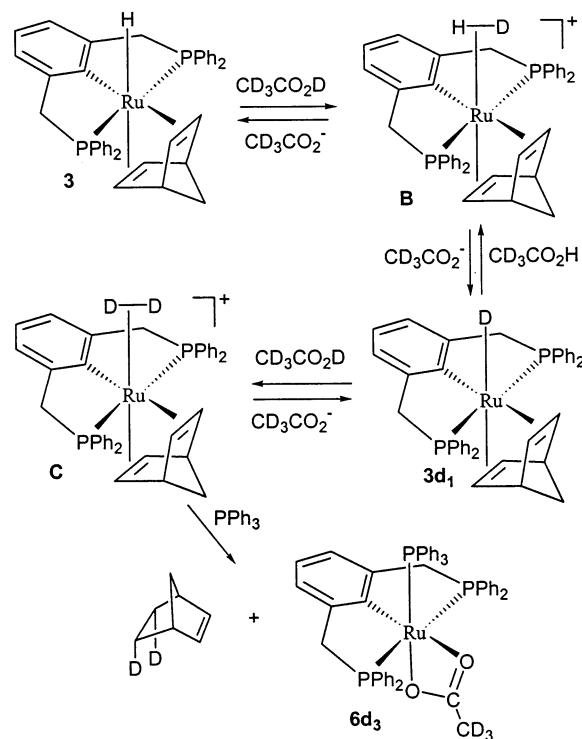
Table 3. Selected Bond Lengths (Å) and Bond Angles (deg) for [Ru(OAc)(PPh₃)(PCP)] (6**)**

Ru(1)–P(1)	2.3271(6)	Ru(1)–P(2)	2.3154(6)
Ru(1)–P(3)	2.2862(6)	Ru(1)–C(1)	2.045(2)
Ru(1)–O(1)	2.1688(15)	Ru(1)–O(2)	2.3192(16)
O(1)–C(9)	1.268(3)	O(2)–C(9)	1.259(3)
P(2)–Ru(1)–P(1)	159.70(2)	P(3)–Ru(1)–P(1)	96.76(2)
P(3)–Ru(1)–P(2)	96.13(2)	C(1)–Ru(1)–P(1)	83.25(6)
C(1)–Ru(1)–P(2)	81.30(6)	C(1)–Ru(1)–P(3)	89.22(6)
O(1)–Ru(1)–P(1)	85.20(4)	O(2)–Ru(1)–P(1)	94.18(5)
O(1)–Ru(1)–P(2)	84.79(4)	O(2)–Ru(1)–P(2)	95.49(4)
O(1)–Ru(1)–P(3)	170.11(5)	O(2)–Ru(1)–P(3)	111.88(4)
C(1)–Ru(1)–O(1)	100.64(7)	C(1)–Ru(1)–O(2)	158.89(7)
O(1)–Ru(1)–O(2)	58.24(6)	O(1)–C(9)–C(10)	119.5(2)
O(2)–C(9)–C(10)	120.5(3)	O(2)–C(9)–O(1)	120.0(2)
C(9)–O(1)–Ru(1)	94.19(13)	C(9)–O(2)–Ru(1)	87.54(14)
O(1)–C(9)–Ru(1)	56.60(11)	O(2)–C(9)–Ru(1)	63.42(12)

deuterium is transferred to the NBD ligand from the same side of the metal. The production of [Ru(O₂CCD₃)(PPh₃)(PCP)] (**6d₃**) in the protonation has been confirmed by the ³¹P{¹H} and ¹H NMR spectra.

The acetate complex [Ru(O₂CCH₃)(PPh₃)(PCP)] (**6**) has been prepared alternatively from the reaction of **2** with AgO₂CMe. The structure of **6** has been confirmed by X-ray diffraction. The crystallographic details and selected bond distances and angles are given in Tables 1 and 3, respectively. As shown in Figure 2, complex **6** has a distorted-octahedral structure with a bidentate acetate ligand and a meridionally coordinated PCP ligand. The acetate is unsymmetrically bound to ruthenium with Ru–O distances of 2.1688(15) and 2.3192(16) Å. The O(1)–Ru(1)–O(2) angle (58.24(6)°) is close to those in reported ruthenium complexes with a bidentate carboxylate ligand.²⁹ The P(1)–Ru–P(2) bond angle is 159.70(2)°, which is larger than those in Ru(PCP)

Scheme 3



complexes such as **2** (150.4(1)°), [RuCl(PPh₃)(PCP)] (152.49(2)°),^{18b} and [Ru(PCP)(PCHP)]OTf (153.64(3)°).^{15d} The solid-state structure of **6** is maintained in solution, as suggested by the NMR data. In particular, the ¹H NMR spectrum in C₆D₆ showed virtual triplet signals at 3.24 and 3.82 ppm for the methylene protons of the PCP ligand and a singlet signal at 1.03 ppm for the CH₃ group. The ³¹P{¹H} NMR spectrum in C₆D₆ showed a doublet at 46.8 ppm for PPh₂ and a triplet at 53.4 ppm for PPh₃.

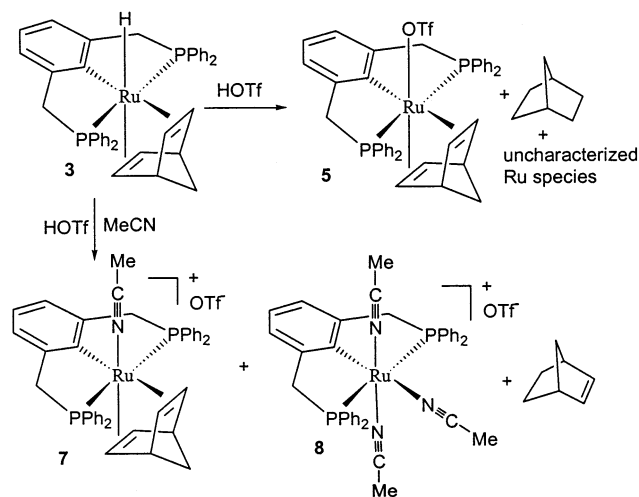
We have monitored the protonation reaction of **3** with CD₃CO₂D by ³¹P{¹H} and ¹H NMR spectroscopy. The experiments reveal that the Ru–H in **3** readily undergoes H/D exchange with CD₃CO₂D to give [RuD(NBD)(PCP)] (**3d₁**) and that the H/D exchange reaction is faster than the hydrogenation reaction. For example, after a mixture of **3** and 5.7 equiv of CD₃CO₂D in CD₂-Cl₂ was allowed to stand for 25 min, about 80% of hydride **3** was converted to [RuD(NBD)(PCP)] and only about 5% [Ru(O₂CCD₃)(PPh₃)(PCP)] (**6d₃**) was produced along with NBE at this stage. After 40 h, complex **3** is completely converted to [Ru(O₂CCD₃)(PPh₃)(PCP)] and partially deuterated NBE (see Scheme 2). As suggested by the ¹H NMR, the endo positions of the NBE generated in the protonation reaction have about 25% of hydrogen and 75% of deuterium. It should be mentioned that we have not been able to detect by NMR spectroscopy any intermediates of the protonation reactions, as the NMR spectra collected during the process only showed the signals of complexes **3**, **3d₁**, **6d₃**, and norbornene.

As mentioned previously, protonation of **3** is expected to give the dihydrogen complex [Ru(H₂)(NBD)(PCP)]⁺. The H/D exchange between **3** with CD₃CO₂D likely involves the intermediate [Ru(HD)(NBD)(PCP)]⁺. As shown in Scheme 3, reaction of **3** with CD₃CO₂D could produce the η²-HD complex [Ru(η²-HD)(NBD)(PCP)]⁺

(28) Laszlo, P.; Schleyer, P. v. R. *J. Am. Chem. Soc.* **1964**, *86*, 1171.

(29) See for example: (a) Sanford, M. S.; Valdez, M. R.; Grubbs, R. H. *Organometallics* **2001**, *20*, 5455. (b) González-Herrero, P.; Weberndörfer, B.; Ilg, K.; Wolf, J.; Werner, H. *Organometallics* **2001**, *20*, 3672. (c) Kuznetsov, V. F.; Yap, G. P. A.; Alper, H. *Organometallics* **2001**, *20*, 1300.

Scheme 4



(**B**), which can then be deprotonated by CD_3CO_2^- to give **3d₁**. Similar mechanisms have been proposed previously, for example, for the H/D exchange of $[\text{W}(\text{D}_2)(\text{CO})_3(\text{P}-\text{Pr})_3]$ with H_2O^{30} and for the H/D exchange of $[\text{Ru}(\text{Tp})(\text{H}_2)(\text{PPh}_3)_2]^+$ with D_2O^{31} .

In the reaction of **3** with $\text{CD}_3\text{CO}_2\text{D}$, the NBE could also be formed through the intermediate $[\text{Ru}(\eta^2\text{-H}_2)(\text{NBD})(\text{PCP})]^+$ or its isotopomers. For example, NBE- d_2 could be formed from $[\text{Ru}(\eta^2\text{-D}_2)(\text{NBD})(\text{PCP})]^+$ (**C**) (Scheme 3). Such a proposition is consistent with the fact that protonation of **3** with $\text{CD}_3\text{CO}_2\text{D}$ gives deuterated NBE in which the deuterium atoms are at the endo positions of NBE. The fact that the NBD ligand of **3** can only be hydrogenated slowly and that **3** and/or **3d₁** are the only NMR-observable species before hydrogenation even in the presence of excess acetic acid suggests that the acidity of acetic acid is not strong enough to generate the dihydrogen intermediate in a substantial amount.

Protonation of 3 with HOTf. If the intermediate $[\text{Ru}(\text{H}_2)(\text{NBD})(\text{PCP})]^+$ is involved in the hydrogenation of the NBD ligand, one would expect that protonation of **3** with a stronger acid should speed up the reaction. To test this idea, we have studied the protonation reaction of **3** with the strong acid HOTf in CD_2Cl_2 . As confirmed by NMR, **3** indeed reacted with HOTf rapidly at room temperature to give $[\text{Ru}(\text{OTf})(\text{NBD})(\text{PCP})]$ (**5**) and norbornane along with some uncharacterized phosphorus-containing species (Scheme 4). Formation of $[\text{Ru}(\text{OTf})(\text{NBD})(\text{PCP})]$ in the protonation reaction strongly suggests that the dihydrogen complex $[\text{Ru}(\text{H}_2)(\text{NBD})(\text{PCP})]\text{OTf}$ was produced as the initial product in the protonation reaction. One can easily see that displacement of the H_2 ligand in $[\text{Ru}(\text{H}_2)(\text{NBD})(\text{PCP})]\text{OTf}$ by OTf^- can lead to $[\text{Ru}(\text{OTf})(\text{NBD})(\text{PCP})]$. Production of norbornane in the protonation reaction can also be related to the dihydrogen complex. The dihydrogen intermediate $[\text{Ru}(\text{H}_2)(\text{NBD})(\text{PCP})]\text{OTf}$ may undergo hydrogen transfer from the H_2 to the NBD ligand to give $[\text{Ru}(\text{OTf})(\text{NBE})(\text{PCP})]$, which then reacts with a H_2 molecule released from the formation of $[\text{Ru}(\text{OTf})(\text{NBD})(\text{PCP})]$ to give the fully hydrogenated product norbornane and the unsaturated $[\text{Ru}(\text{PCP})]^+$ fragment. We have attempted to detect the dihydrogen intermediate

by monitoring the protonation reaction at 225 K by NMR. However, the reaction is too fast, and only $[\text{Ru}(\text{OTf})(\text{NBD})(\text{PCP})]$ (**4**) was identified as the major phosphorus-containing product under the reaction conditions.

Reaction of $[\text{Ru}(\text{OTf})(\text{NBD})(\text{PCP})]$ with H_2 . If norbornane were formed from the dihydrogen intermediate $[\text{Ru}(\text{H}_2)(\text{NBD})(\text{PCP})]\text{OTf}$, one would expect that reaction of $[\text{Ru}(\text{OTf})(\text{NBD})(\text{PCP})]$ with H_2 should also produce norbornane. Indeed, such an expectation has been confirmed experimentally. As indicated by ^1H NMR, norbornane was generated when a CD_2Cl_2 solution of $[\text{Ru}(\text{OTf})(\text{NBD})(\text{PCP})]$ was exposed to H_2 for 20 min. We have also monitored the hydrogenation process by NMR. Again, the ^1H and $^{31}\text{P}\{^1\text{H}\}$ NMR spectra collected during the process only show the signals of the starting material $[\text{Ru}(\text{OTf})(\text{NBD})(\text{PCP})]$ and final products. In other words, under a H_2 atmosphere, $[\text{Ru}(\text{OTf})(\text{NBD})(\text{PCP})]$ rather than $[\text{Ru}(\text{H}_2)(\text{NBD})(\text{PCP})]^+$ is the NMR-observable species before hydrogenation. The results suggest that the affinity of OTf^- to $[\text{Ru}(\text{NBD})(\text{PCP})]^+$ is higher than that of H_2 and that hydrogen transfer can occur readily to give hydrogenated product once $[\text{Ru}(\text{H}_2)(\text{NBD})(\text{PCP})]^+$ is formed. The lower affinity of H_2 for the $[\text{Ru}(\text{NBD})(\text{PCP})]^+$ fragment together with the high reactivity of $[\text{Ru}(\text{H}_2)(\text{NBD})(\text{PCP})]^+$ prevents us from detecting $[\text{Ru}(\text{H}_2)(\text{NBD})(\text{PCP})]^+$ by NMR experiments.

It should be noted that we were unable to characterize the metal-containing products in the reaction. After a CD_2Cl_2 solution of $[\text{Ru}(\text{OTf})(\text{NBD})(\text{PCP})]$ was exposed to H_2 for 20 min, the $^{31}\text{P}\{^1\text{H}\}$ NMR spectrum showed several new peaks likely associated with solvated $[\text{Ru}(\text{PCP})]^+$ species. Indeed, addition of CD_3CN to the reaction mixture produced $[\text{Ru}(\text{CD}_3\text{CN})_3(\text{PCP})]^+$. However, if a CD_2Cl_2 solution of $[\text{Ru}(\text{OTf})(\text{NBD})(\text{PCP})]$ was exposed to H_2 for 18 h, all the starting material $[\text{Ru}(\text{OTf})(\text{NBD})(\text{PCP})]$ was consumed and only norbornane could be identified. The $^{31}\text{P}\{^1\text{H}\}$ and ^1H signals associated with the metal-containing products are featureless.

Protonation of 3 with HOTf in the Presence of CH_3CN . In a further effort to verify that the dihydrogen complex $[\text{Ru}(\text{H}_2)(\text{NBD})(\text{PCP})]\text{OTf}$ is the most likely initial product in the protonation reaction of **3** with HOTf, we have protonated $[\text{Ru}(\text{H}_2)(\text{NBD})(\text{PCP})]\text{OTf}$ with HOTf in the presence of acetonitrile. It is expected that $[\text{Ru}(\text{MeCN})(\text{NBD})(\text{PCP})]\text{OTf}$ (**7**) would be produced if $[\text{Ru}(\text{H}_2)(\text{NBD})(\text{PCP})]\text{OTf}$ were formed in the protonation reaction. In dichloromethane in the presence of acetonitrile, **3** reacted with HOTf, giving $[\text{Ru}(\text{MeCN})(\text{NBD})(\text{PCP})]\text{OTf}$ (**7**) and $[\text{Ru}(\text{MeCN})_3(\text{PCP})]^+$ (**8**) along with NBE, as confirmed by NMR spectroscopy (Scheme 4).

The complex $[\text{Ru}(\text{MeCN})(\text{NBD})(\text{PCP})]\text{OTf}$ (**7**) has been synthesized alternatively from the reaction of $[\text{Ru}(\text{OTf})(\text{NBD})(\text{PCP})]$ with acetonitrile. The structure of **7** has been confirmed by an X-ray diffraction study. The molecular structure of **7** is depicted in Figure 3. The crystallographic details and selected bond distances and angles are given in Tables 1 and 4, respectively. The structure of **7** can be described as a distorted octahedron with an CH_3CN ligand trans to one of the double bonds of NBD. The structural features associated with PCP and NBD in complex **7** are very similar to those of complex **2**. The Ru–N(1) and N(1)–C(61) bond distances

(30) Kubas, G. J.; Burns, C. J.; Khalsa, G. R. K.; Van der Sluys, L. S.; Kiss, G.; Hoff, C. D. *Organometallics* **1992**, *11*, 3390.

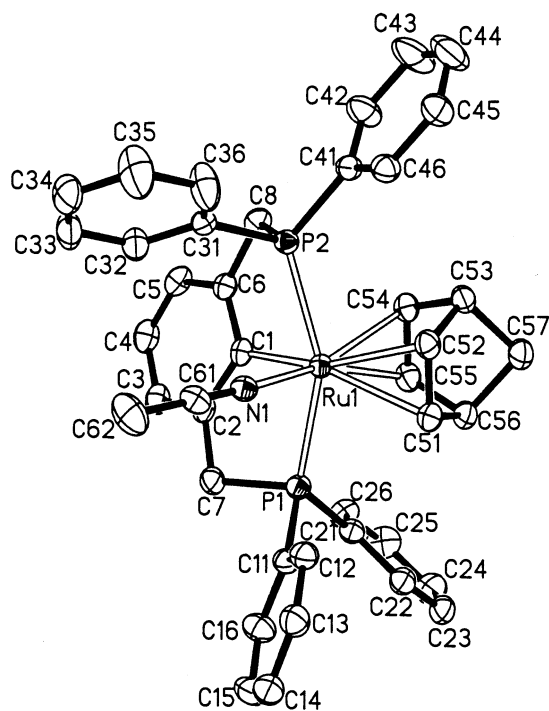


Figure 3. Molecular structure of [Ru(MeCN)(NBD)(PCP)]⁺. Hydrogen atoms are omitted for clarity.

Table 4. Selected Bond Lengths (Å) and Bond Angles (deg) for [Ru(MeCN)(NBD)(PCP)]OTf (7)

Ru(1)–P(1)	2.3642(11)	Ru(1)–P(2)	2.3721(11)
Ru(1)–C(1)	2.109(4)	Ru(1)–N(1)	2.044(3)
Ru(1)–C(51)	2.323(4)	Ru(1)–C(52)	2.311(4)
Ru(1)–C(54)	2.223(4)	Ru(1)–C(55)	2.225(4)
N(1)–C(61)	1.133(5)	C(61)–C(62)	1.451(6)
C(51)–C(52)	1.365(6)	C(54)–C(55)	1.379(6)
C(52)–C(53)	1.533(6)	C(53)–C(54)	1.535(6)
C(55)–C(56)	1.551(6)	C(51)–C(56)	1.538(6)
C(53)–C(57)	1.555(6)	C(56)–C(57)	1.539(6)
P(1)–Ru(1)–P(2)	153.63(4)	N(1)–Ru(1)–C(1)	90.93(13)
C(1)–Ru(1)–P(1)	80.38(12)	N(1)–Ru(1)–P(1)	81.44(9)
C(1)–Ru(1)–P(2)	77.47(11)	N(1)–Ru(1)–P(2)	84.79(9)
C(1)–Ru(1)–C(51)	154.40(15)	N(1)–Ru(1)–C(51)	104.26(14)
C(1)–Ru(1)–C(52)	160.32(16)	N(1)–Ru(1)–C(52)	102.59(14)
C(1)–Ru(1)–C(54)	99.36(15)	N(1)–Ru(1)–C(54)	157.08(14)
C(1)–Ru(1)–C(55)	96.83(15)	N(1)–Ru(1)–C(55)	162.38(15)
C(61)–N(1)–Ru(1)	175.4(3)	N(1)–C(61)–C(62)	179.5(5)

and Ru(1)–N(1)–C(61) angle (175.4(3)°) are similar to those in acetonitrile complexes such as [Ru(Cp)(CH₃CN)₂(PR₃)⁺ (R = Cy, Me)^{31a} and [Ru(2,9-dimethyl-1,10-phenanthroline)₂(CH₃CN)₂](PF₆)₂.^{31b} The solid-state structure is fully supported by the NMR data. The structure of complex **8** is proposed on the basis of the NMR data. In particular, the ³¹P{¹H} NMR spectrum displayed a singlet at 49.5 ppm. The ¹H NMR spectrum showed a virtual triplet for the methylene protons of PCP at 3.98 ppm, indicating that the complex has a symmetric structure with a meridionally bound PCP ligand.

Formation of [Ru(MeCN)(NBD)(PCP)]OTf is consistent with the proposition that [Ru(H₂)(NBD)(PCP)]OTf was initially produced in the protonation reaction, as [Ru(MeCN)(NBD)(PCP)]OTf can be thought of as being

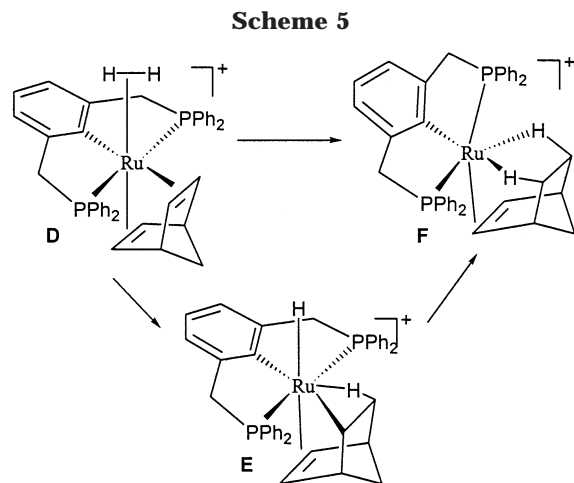
formed by displacement of the H₂ ligand in [Ru(H₂)(NBD)(PCP)]OTf with MeCN. Apparently, some of the [Ru(H₂)(NBD)(PCP)]OTf also undergoes a hydrogen transfer reaction in the presence of MeCN to give norbornene and [Ru(MeCN)₃(PCP)]⁺. In agreement with the proposition, protonation of **3** with DOTf in the presence of CD₃CN produced partially deuterated NBE in which the deuteriums are at the endo positions. It is understandable that norbornene rather than norbornane was formed in the protonation reaction, because norbornene can be displaced by acetonitrile before it can be hydrogenated further to norbornane.

Comments on the Protonation Reactions. We have studied the protonation reactions of [RuH(NBD)(PCP)] with acetic acid and HOTf. The products of the protonation reactions are dependent on the acids used and reaction conditions. For example, protonation of [RuH(NBD)(PCP)] with acetic acid in the presence of PPh₃ gives norbornene and [Ru(OAc)(PPh₃)(PCP)], protonation of [RuH(NBD)(PCP)] with HOTf gives norbornane and [Ru(OTf)(NBD)(PPh₃)(PCP)], and protonation of [RuH(NBD)(PCP)] with HOTf in the presence of MeCN gives norbornene, [Ru(MeCN)(NBD)(PCP)]OTf, and [Ru(MeCN)₃(PCP)]OTf. All the products can be related to the reactive dihydrogen intermediate [Ru(H₂)(NBD)(PCP)]⁺.

It is noted that [Ru(OTf)(NBD)(PCP)] and [Ru(MeCN)(NBD)(PCP)]OTf were produced when [RuH(NBD)(PCP)] was protonated with HOTf in the absence or presence of MeCN. However, [Ru(OAc)(NBD)(PCP)] was not produced in the protonation of [RuH(NBD)(PCP)] with acetic acid. The difference may be related to the basicities of OAc[−] and OTf[−]. As mentioned previously, when [RuH(NBD)(PCP)] was treated with CD₃CO₂D, [RuH(NBD)(PCP)] undergoes an H/D exchange reaction with CD₃CO₂D to give [RuD(NBD)(PCP)], and [RuX(NBD)(PCP)] (X = H, D) are the only NMR-observable species before hydrogenation. These observations suggest that the acidity of acetic acid is not strong enough to generate a substantial amount of [Ru(H₂)(NBD)(PCP)]⁺ but acetate anion can function as a base to deprotonate the dihydrogen complex [Ru(H₂)(NBD)(PCP)]⁺, if generated, to give back the hydride complex [RuH(NBD)(PCP)]. In other words, acetate will deprotonate [Ru(H₂)(NBD)(PCP)]⁺ rather than displace the H₂ ligand. Thus, [Ru(OAc)(NBD)(PCP)] was not produced when **3** is treated with acetic acid. On the other hand, HOTf is a strong acid that can protonate **3** completely to give the dihydrogen complex [Ru(H₂)(NBD)(PCP)]⁺ and OTf[−] is a weak base that could not deprotonate the dihydrogen complex. Once the dihydrogen complex [Ru(H₂)(NBD)(PCP)]⁺ was formed, the dihydrogen ligand could be readily displaced. Therefore, [Ru(OTf)(NBD)(PCP)] and [Ru(MeCN)(NBD)(PCP)]OTf were produced when **3** was treated with HOTf.

The experimental results described above strongly suggest that the dihydrogen complex [Ru(H₂)(NBD)(PCP)]⁺ is the active species in the hydrogenation of the coordinated NBD ligand. Scheme 5 summarizes the possible reaction pathways for the hydrogenation process. The hydrogen transfer from the coordinated H₂ to the NBD ligand of [Ru(H₂)(NBD)(PCP)]⁺ (**D**) could go through a concerted mechanism (path B) or through a stepwise one in which one of the hydrogens from the

(31) (a) Rüba, E.; Simanko, W.; Mauthner, K.; Soldouzi, K. M.; Slugovc, K.; Mereiter, K.; Schmid, K.; Kirchner, K. *Organometallics* **1999**, *18*, 3843. (b) Pezet, F.; Daran, J. C.; Sasaki, I.; Ait-Haddou, H.; Balavoine, G. G. A. *Organometallics* **2000**, *19*, 4008.



coordinated H_2 is transferred to the NBD to give the hydrido alkyl complex $[\text{RuH}(\text{C}_7\text{H}_9)(\text{PCP})]^+$ (**E**) followed by reductive elimination (path A). Scheme 5 does not consider the involvement of the $\text{PPh}_3/\text{CH}_3\text{CN}$ coordination. This is justified, because additional ligands are not necessary for the hydrogenation to occur. As supporting evidence, the NBD ligand of $\text{RuH}(\text{NBD})(\text{PCP})$ is hydrogenated when treated with HOTf without addition of other ligands.

Computational Study. Scheme 5 gives two possible reaction pathways for the hydrogenation process. The detailed pathways for the hydrogen transfer process, however, could not be determined experimentally. To examine the feasibility of the two proposed reaction pathways, the structural and energetic aspects of the possible reaction pathways for the conversion of the complex $[\text{Ru}(\text{H}_2)(\text{NBD})(2,6-(\text{H}_2\text{PCH}_2)_2\text{C}_6\text{H}_3)]^+$ (**9**) to the assumed product $[\text{Ru}(\text{NBE})(2,6-(\text{H}_2\text{PCH}_2)_2\text{C}_6\text{H}_3)]^+$ (**11**) have been studied by density functional calculations at the B3LYP level of theory. Here, **9** and **11** are the model complexes of **D** and **F** proposed in Scheme 5, respectively. We also hope to clarify whether the hydrogenation goes through a stepwise or concerted mechanism.

When the one-step concerted pathway was considered, attempts to locate the transition state were not successful. We have explored the potential energy surface in the vicinity of the possible concerted transition structure. In doing so, we obtained a series of partially optimized structures having various predefined $\text{H}\cdots\text{C}$ distances. Here, H denotes the transferring hydrogens and C denotes the hydrogen-receiving carbons of the coordinated NBD ligand. Among these partially optimized structures, the highest energy structure along the concerted reaction coordinate has the two $\text{H}\cdots\text{C}$ distances at 1.585 Å and is 70 kcal/mol above the dihydrogen complex **9**. Frequency calculations based on this structure give three imaginary frequencies (-1060.6 , -704.3 , and -9.4 cm^{-1}). The two larger imaginary frequencies correspond to the asymmetric and symmetric motions of the two transferring hydrogens along the direction of the concerted reaction coordinate. In view of the high-energy area in the vicinity of the possible transition structure for the concerted pathway and the frequency calculations discussed above, we can conclude that a transition state corresponding to the one-step hydrogenation does not exist. Thus, conversion of **9** to **11** through a concerted process is unlikely.

On the other hand, the calculations suggest that conversion of **9** to **11** through a stepwise process is feasible. Figure 4 shows the reaction steps for the conversion of **9** to **11** through **10** (the model complex of **E** proposed in Scheme 5), together with the relative free energies and reaction energies (in parentheses) calculated for all the species. It is clear that the relative free energies do not differ too much from the relative reaction energies. Our calculations are based on the gas-phase model. The calculated results are used to simulate the reactions in solution. Therefore, relative free energies that consider the entropy effect and thermal/zero-point energy corrections will be used in the following discussion.

As shown in Figure 4, the stepwise mechanism involves two steps: one hydrogen atom from the coordinated H_2 is transferred to NBD to form intermediate **10** through transition state **TS1** with a barrier of 19.08 kcal/mol, and then the second hydrogen transfer completes the hydrogenation of one of the two double bonds of NBD to form the NBE complex **11**. The barrier of the second hydrogen transfer is only 6.77 kcal/mol. The first hydrogen transfer is therefore the rate-determining step in the reaction. After the rate-determining barrier is surmounted, the reaction proceeds easily by having the second hydrogen transfer. The conversion from **9** to **11** is exothermic and irreversible. In view of the large energy difference between **9** and **11** and the small barriers connecting them, it is not too surprising that the dihydrogen complex $[\text{Ru}(\text{H}_2)(\text{NBD})(\text{PCP})]^+$ was not detected in the experiments.

Figure 5 shows the optimized structures with selected structural parameters for all the related species. Complex **9** is a typical octahedral dihydrogen complex with a short H–H distance of 0.868 Å. The first transition state (**TS1**) corresponds to a dihydride species in which one of the hydrides is 1.645 Å from the receiving carbon of NBD. The intermediate **10** can be described as a pentagonal bipyramid (PB) in which one hydride and one olefin ligand form the axle of the PB structure and the PCP and agostic ligand lie on the equatorial plane. The intermediate is formally seven-coordinated with a Ru(IV) center. An osmium analogue, the formally seven-coordinated Os(IV) complex $[\text{OsH}_2(\eta^3\text{-C}_6\text{H}_9)(\text{P}(i\text{-Pr})_3)_2]^+$ with an agostic interaction, has recently been reported by Esteruelas et al.¹³ Interestingly, when the second hydrogen is transferred to form **11**, the PCP ligand changes from a meridional arrangement to a facial arrangement. The P–Ru–P angles in **9** and **10** are 157.3 and 149.8°, respectively. However, the P–Ru–P angles become 100.7 and 101.7° in **TS2** and **11**, respectively. The facial arrangement of a PCP ligand is not unusual, as some Os complexes with a facially coordinated PCP ligand have been characterized by X-ray diffraction in our laboratory.³² In addition, the aryldiamine ligand 2,6-(Me_2NCH_2)₂ C_6H_3 , which is analogous to PCP, adopts a pseudofacial arrangement in the complexes $[\text{RuX}(\text{NBD})-(2,6-(\text{Me}_2\text{NCH}_2)_2\text{C}_6\text{H}_3)]$ (X = Cl, OTf; see structure **A** in Scheme 1 for their geometry).²⁴ The facial arrangement of the PCP ligand in **TS2** and **11** can be related to the special structural features of the agostic NBE ligand.

Summary and Concluding Remarks. We have prepared the hydride complex $[\text{RuH}(\text{NBD})(\text{PCP})]$ and

(32) Wen, T. B.; Zhou, Z. Y.; Jia, G. Unpublished results.

(ii) protonation of $[\text{RuH}(\text{NBD})(\text{PCP})]$ in the presence of MeCN produced $[\text{Ru}(\text{MeCN})(\text{NBD})(\text{PCP})]^+$, (iii) protonation of $[\text{RuH}(\text{NBD})(\text{PCP})]$ with deuterated acids produced partially deuterated norbornene in which the deuterium is only incorporated at the endo position, (iv) hydrogenated product was obtained when $[\text{Ru}(\text{OTf})(\text{NBD})(\text{PCP})]$ was treated with H_2 , and (v) the computational study confirms that $[\text{Ru}(\text{H}_2)(\text{NBD})(\text{PCP})]^+$ is a reasonable species. The computational study also suggests that hydrogen transfer from the dihydrogen to the NBD ligand of $[\text{Ru}(\text{H}_2)(\text{NBD})(\text{PCP})]^+$ most likely proceeds by first transferring one of the hydrogens from the coordinated H_2 to the NBD to give the hydrido alkyl complex $[\text{RuH}(\text{C}_7\text{H}_9)(\text{PCP})]^+$, which is then followed by reductive elimination.

We have previously shown that protonation of $[\text{Ru}(\text{Cp}^*)\text{H}(\text{NBD})]$ produces nortricyclene through the dihydrogen intermediate $[\text{Ru}(\text{Cp}^*)(\text{H}_2)(\text{NBD})]^+$, where H_2 is cis to both of the double bonds of NBD.^{12a} In this regard, it is interesting to note that norbornene is produced when $[\text{RuH}(\text{NBD})(\text{PCP})]$ is protonated. The latter reaction may involve the dihydrogen complex $[\text{Ru}(\text{H}_2)(\text{NBD})(\text{PCP})]^+$, where H_2 is only cis to one of the double bonds of NBD. It has also been suggested that norbornene and nortricyclene can be formed from *mer*- and *fac*- $[\text{M}(\text{H}_2)(\eta^4\text{-NBD})(\text{CO})_3]$ ($\text{M} = \text{Cr}, \text{Mo}, \text{W}$), respectively.¹⁰ These results suggest that the relative positions of the NBD olefinic functions to that of the H_2 ligand are important in determining the structures of the hydrogenation products (norbornene and nortricyclene).

Experimental Section

All manipulations were carried out at room temperature under a nitrogen atmosphere using standard Schlenk techniques, unless otherwise stated. Solvents were distilled under nitrogen from sodium–benzophenone (hexane, diethyl ether, THF, benzene) or calcium hydride (dichloromethane, CHCl_3). The starting material $[\text{RuCl}(\text{PPh}_3)(\text{PCP})]$ was prepared according to a literature method.^{18b} Microanalyses were performed by M-H-W Laboratories (Phoenix, AZ). ^1H , $^{13}\text{C}\{^1\text{H}\}$, and $^{31}\text{P}\{^1\text{H}\}$ NMR spectra were collected on a Bruker ARX-300 spectrometer (300 MHz). ^1H and ^{13}C NMR chemical shifts are relative to TMS, and ^{31}P NMR chemical shifts are relative to 85% H_3PO_4 .

$[\text{RuCl}(\text{NBD})(\text{PCP})]$ (2). A mixture of $[\text{RuCl}(\text{PPh}_3)(\text{PCP})]$ (1.70 g, 1.95 mmol), NBD (1.0 mL, 9.8 mmol), and CuCl (1.0 g, 10 mmol) in CH_2Cl_2 (90 mL) was stirred for 6 h. The insoluble material was then removed by filtration through Celite, and the volume of the filtrate was reduced to ca. 3 mL. Addition of hexane (60 mL) to the residue caused precipitation of a greenish yellow solid. The solid was collected by filtration, washed with hexane (2×10 mL), and dried under vacuum overnight. Yield: 1.1 g, 80%. Anal. Calcd for $\text{C}_{39}\text{H}_{35}\text{ClP}_2\text{Ru}$: C, 66.71; H, 5.02. Found: C, 66.70; H, 4.94. ^1H NMR (300.13 MHz, C_6D_6): δ 0.65 (d, $J(\text{HH}) = 8.0$ Hz, 1H, CHH), 0.88 (d, $J(\text{HH}) = 8.0$ Hz, 1H, CHH), 2.70 (s, 2H, CH), 2.90 (s, 2H, =CH), 4.20 (m, 2H, CH_2P), 4.32 (m, 2H, CH_2P), 4.94 (s, 2H, =CH), 7.22 (br m, 12H, PPh_2), 8.02 (br m, 8H, PPh_2). $^{31}\text{P}\{^1\text{H}\}$ NMR (121.49 MHz, C_6D_6): δ 55.4 (s).

$[\text{Ru}(\text{O}_2\text{CH})(\text{NBD})(\text{PCP})]$ (4). A mixture of **2** (0.25 g, 0.36 mmol) and TlO_2CH (0.25 g, 1.0 mmol) in THF (30 mL) was stirred for 4 h. The THF was then removed under vacuum. To the residue was added benzene (30 mL). The mixture was stirred for 15 min and then filtered through Celite. The volume of the filtrate was reduced to ca. 3 mL under vacuum. Addition of hexane (60 mL) to the residue produced a yellow solid, which was collected by filtration, washed with hexane, and dried

under vacuum. Yield: 0.21 g, 82%. Anal. Calcd for $\text{C}_{40}\text{H}_{36}\text{O}_2\text{P}_2\text{Ru}$: C, 67.50; H, 5.10. Found: C, 67.54; H, 5.26. ^1H NMR (300.13 MHz, C_6D_6): δ 0.56 (d, $J(\text{HH}) = 8.2$ Hz, 1H, CHH), 0.91 (d, $J(\text{HH}) = 8.2$ Hz, 1H, CHH), 2.67 (s, 2H, CH), 2.74 (s, 2H, =CH), 4.16 (m, 2H, CH_2P), 4.27 (m, 2H, CH_2P), 5.97 (s, 2H, =CH), 7.11–7.76 (m, 20H, PPh_2), 7.97 (s, 1H, O_2CH). $^{31}\text{P}\{^1\text{H}\}$ NMR (121.49 MHz, C_6D_6): δ 59.4 (s).

$[\text{Ru}(\text{OTf})(\text{NBD})(\text{PCP})]$ (5). A mixture of **2** (1.0 g, 1.4 mmol) and TlOTf (1.0 g, 2.8 mmol) in CH_2Cl_2 (60 mL) was stirred for 1.5 h. The insoluble TlCl was removed by filtration. The volume of the filtrate was reduced to ca. 3 mL under vacuum. Addition of hexane (30 mL) to the residue produced a brownish yellow solid, which was collected by filtration, washed with hexane, and dried under vacuum overnight. Yield: 1.0 g, 86%. ^1H NMR (300.13 MHz, CD_2Cl_2): δ 0.75 (br s, 1H, CH_2), 0.96 (br s, 1H, CH_2), 2.64 (s, 2H, CH), 2.73 (s, 2H, =CH), 4.26 (br, 2H, CH_2P), 4.45 (br, 2H, CH_2P), 5.50 (s, 2H, =CH), 7.27–8.12 (m, 20H, PPh_2). $^{31}\text{P}\{^1\text{H}\}$ NMR (121.49 MHz, CD_2Cl_2): δ 55.2 (br s).

$[\text{RuH}(\text{NBD})(\text{PCP})]$ (3). Method A. A mixture of **5** (0.70 g, 0.86 mmol) and NaBH_4 (0.30 g, 7.9 mmol) in THF (60 mL) was stirred at room temperature for 1 h. The mixture was filtered through Celite. The solvent of the filtrate was removed completely. Addition of MeOH (60 mL) to the residue produced a brownish yellow solid, which was collected by filtration, washed with MeOH (3×10 mL), and dried under vacuum overnight to give pure **3**. Yield: 0.45 g, 79%.

Method B. A mixture of **2** (0.20 g, 0.28 mmol) and NaBH_4 (0.10 g, 2.63 mmol) in THF (30 mL) was refluxed for 8 h. The solvent was then removed completely, and the residue was extracted with benzene (20 mL). The volume of the extract was reduced to 3 mL. Addition of hexane (20 mL) to the residue produced a brownish yellow solid, which was collected by filtration, washed with hexane and MeOH, and dried under vacuum overnight to give 0.095 g of crude product. The NMR spectra show that the crude product contains mainly complex **3** along with other unidentified phosphorus-containing species.

Method C. A solution of **4** (0.02 g, 0.028 mmol) in C_6D_6 in an NMR tube was heated for 16 h. Then NMR spectra were collected. The NMR spectra show that **3** was produced along with some minor phosphorus-containing species. Characterization data for **3** are as follows. Anal. Calcd for $\text{C}_{39}\text{H}_{36}\text{P}_2\text{Ru}$: C, 70.15; H, 5.43. Found: C, 70.15; H, 5.59. ^1H NMR (300.13 MHz, CD_2Cl_2): δ -11.53 (t, $J(\text{PH}) = 22.5$ Hz, 1H, RuH), 0.56 (s, 2H, CH_2), 2.23 (s, 2H, CH), 3.16 (s, 2H, =CH), 3.44 (s, 2H, =CH), 3.73 (br d, $J(\text{HH}) = 15.9$ Hz, 2H, CH_2P), 4.47 (br d, $J(\text{HH}) = 15.9$ Hz, 2H, CH_2P), 7.26–7.80 (m, 20H, PPh_2). $^{31}\text{P}\{^1\text{H}\}$ NMR (121.49 MHz, CD_2Cl_2): δ 76.9 (s). $^{13}\text{C}\{^1\text{H}\}$ NMR (75.5 MHz, CD_2Cl_2): δ 47.2 (t, $J(\text{PC}) = 16.2$ Hz, CH_2P), 48.2 (s, bridgehead CH), 54.0 (s, =CH), 58.5 (s, =CH), 60.3 (s, CH_2), 127–134 (m, Ph).

$[\text{Ru}(\text{O}_2\text{CMe})(\text{PPh}_3)(\text{PCP})]$ (6). A mixture of **2** (0.16 g, 0.18 mmol) and TlOAc (0.20 g, 0.76 mmol) in CH_2Cl_2 (35 mL) was stirred for 1 h. The TlCl was removed by filtration. The volume of the filtrate was reduced to ca. 3 mL under vacuum. Addition of hexane (30 mL) to the residue produced a yellow solid, which was collected by filtration, washed with hexane, and dried under vacuum. Yield: 0.14 g, 88%. Anal. Calcd for $\text{C}_{52}\text{H}_{45}\text{O}_2\text{P}_3\text{Ru}$: C, 69.71; H, 5.06; Found: C, 69.90; H, 5.13. ^1H NMR (300.13 MHz, C_6D_6): δ 1.03 (s, 3H, CH_3), 3.24 (dt, $J(\text{HH}) = 16.8$ Hz, $J(\text{PH}) = 4.3$ Hz, 2H, CH_2P), 3.82 (dt, $J(\text{HH}) = 16.8$ Hz, $J(\text{PH}) = 5.6$ Hz, 2H, CH_2P), 6.81–7.41 (m, 35H, PPh_2 , PPh_3). $^{31}\text{P}\{^1\text{H}\}$ NMR (121.49 MHz, C_6D_6): δ 46.8 (d, $J(\text{PP}) = 30.0$ Hz), 53.4 (t, $J(\text{PP}) = 30.0$ Hz).

$[\text{Ru}(\text{CH}_3\text{CN})(\text{NBD})(\text{PCP})]\text{OTf}$ (7). A mixture of **5** (0.70 g, 0.86 mmol) and CH_3CN (1 mL) in CH_2Cl_2 (35 mL) was stirred for 2 h. The volume of the reaction mixture was reduced to ca. 3 mL. Addition of hexane (60 mL) to the residue caused precipitation of a yellow solid. The solid was collected by filtration, washed with hexane (2×10 mL), and dried under vacuum overnight. Yield: 0.60 g, 81%. Anal. Calcd for $\text{C}_{42}\text{H}_{38}\text{F}_3\text{-}$

NO₃P₂SRu: C, 58.88; H, 4.47; N, 1.64. Found: C, 58.66; H, 4.63; N, 1.65. ¹H NMR (300.13 MHz, CD₂Cl₂): δ 0.69 (d, *J*(HH) = 8.9 Hz, 1H, C/H), 0.90 (d, *J*(HH) = 8.9 Hz, 1H, CH/H), 1.35 (s, 3H, CH₃), 2.52 (s, 2H, CH), 2.99 (s, 2H, =CH), 4.06 (m, 2H, CH₂P), 4.46 (m, 2H, CH₂P), 5.19 (s, 2H, =CH), 7.35–8.02 (m, 20H, PPh₂). ³¹P{¹H} NMR (121.49 MHz, CD₂Cl₂): δ 54.4 (s).

Protonation of [RuH(NBD)(PCP)] with CD₃CO₂D in the Presence of PPh₃ in CD₂Cl₂ and Identification of NBE by ¹H NMR. In an NMR tube charged with [RuH(NBD)(PCP)] (20 mg, 0.030 mmol), PPh₃ (20 mg, 0.076 mmol), and CD₂Cl₂ (0.7 mL) was added CD₃CO₂D (10 μL, 0.17 mmol) through a microsyringe. The mixture was allowed to stand for 40 h. ¹H and ³¹P{¹H} NMR spectra were then collected. The NMR spectra showed that [Ru(O₂CCD₃)(PPh₃)(PCP)] and partially deuterated norbornene were present. NMR signals of [Ru(O₂CCD₃)(PPh₃)(PCP)] are as follows. ³¹P{¹H} NMR (121.49 MHz, CD₂Cl₂): δ 44.8 (d, *J*(PP) = 30.5 Hz, PCP of [Ru(O₂CCD₃)(PPh₃)(PCP)]), 53.2 (t, *J*(PP) = 30.5 Hz, PPh₃ of [Ru(O₂CCD₃)(PPh₃)(PCP)]). ¹H NMR (300.13 MHz, CD₂Cl₂): δ 3.25 (dt, *J*(HH) = 16.8 Hz, *J*(PH) = 4.3 Hz, 2H, CH₂P), 3.81 (dt, *J*(HH) = 16.8 Hz, *J*(PH) = 5.6 Hz, 2H, CH₂P), 7.24–8.12 (m, Ph). NMR signals of NBE are as follows. ¹H NMR (300.13 MHz, CD₂Cl₂): δ 0.95 (s, 0.5 H, residual endo-H, most of the H at this position has been replaced with deuterium), 1.20 (d, *J*(HH) = 8.1 Hz, 1H, CH₂), 1.41 (d, *J*(HH) = 8.1 Hz, 1H, CH₂), 1.71 (s, 2H, exo-H), 2.93 (s, 2H, CH), 6.10 (s, 2H, =CH). The volatile portion of the reaction mixture can be separated by vacuum transfer. The ¹H NMR spectrum of the vacuum-transferred solution indicates that norbornene is the only volatile organic product formed in the reaction and that the endo positions of NBE obtained under the reaction conditions have about 25% of H and 75% of D.

Protonation of [RuH(NBD)(PCP)] with CD₃CO₂D in the Presence of PPh₃ in CH₂Cl₂ and Identification of Deuterated NBE by ²H NMR. In an NMR tube charged with [RuH(NBD)(PCP)] (20 mg, 0.030 mmol), PPh₃ (20 mg, 0.076 mmol), and CH₂Cl₂ (0.7 mL) was added CD₃CO₂D (10 μL, 0.17 mmol) through a microsyringe. The mixture was allowed to stand for 40 h. After the solution was treated with NaOH, the volatile portion of the reaction mixture was separated by vacuum transfer. The ²H NMR spectrum (61.25 MHz, CH₂Cl₂) of the resulting solution showed a singlet at 0.97 ppm.

Protonation of [RuH(NBD)(PCP)] with HOTf in CD₂Cl₂ and Identification of Norbornane by ¹H NMR. In an NMR tube charged with [RuH(NBD)(PCP)] (20 mg, 0.030 mmol) and CD₂Cl₂ (0.5 mL) was added HOTf (5 μL, 0.06 mmol) through a microsyringe. The mixture was allowed to stand for 10 min, and then NMR spectra were collected. The ³¹P{¹H} NMR spectrum (CD₂Cl₂, 121.49 MHz) showed a broad signal at 55.8 ppm assignable to [Ru(OTf)(NBD)(PCP)] and several other signals of unidentified species in the region 35–84 ppm. The ¹H NMR spectrum (CD₂Cl₂, 300.13 MHz) showed signals of [Ru(OTf)(NBD)(PCP)] and norbornane. The ¹H integrations suggest that [Ru(OTf)(NBD)(PCP)] and norbornane are present in a ratio of ca. 1:0.9. Selected ¹H NMR signals of [Ru(OTf)(NBD)(PCP)]: δ 2.54 (br, bridgehead CH of NBD), 2.63 (br, =CH of NBD), 4.09 (br, CH₂ of PCP), 4.25 (br, CH₂ of PCP). ¹H NMR signals of norbornane: δ 1.19 (m, 6H, CH₂), 1.47 (m, 4H, CH₂), 2.19 (br, 2H, bridgehead CH).

Hydrogenation of [Ru(OTf)(NBD)(PCP)]. A CD₂Cl₂ solution (0.5 mL) of [Ru(OTf)(NBD)(PCP)] was generated in situ in an NMR tube by mixing [RuCl(NBD)(PCP)] (20 mg, 0.028 mmol) and AgOTf (10 mg, 0.039 mmol) for 30 min. The mixture was then stored under 1 atm of H₂ for 20 min, and NMR spectra were collected. The NMR spectra showed that [Ru(OTf)(NBD)(PCP)] and norbornane were present in a ratio of ca. 1.1:1 along with several other uncharacterized phosphorus-containing species. NMR spectra were collected again after the mixture was stored under H₂ for 18 h. The ³¹P NMR spectrum shows that [Ru(OTf)(NBD)(PCP)] was no longer present and a complicated mixture of phosphorus-containing

species were produced. The ¹H NMR spectra of the reaction mixtures showed signals of norbornane. The ¹H NMR signals of norbornane appearing in the ¹H NMR spectrum are as follows. ¹H NMR (300.13 MHz, CD₂Cl₂): δ 1.28 (m, 6H, CH₂), 1.57 (m, 4H, CH₂), 2.29 (br, 2H, bridgehead CH).

Protonation of [RuH(NBD)(PCP)] with HOTf in the Presence of CD₃CN in CD₂Cl₂ and Identification of NBE by ¹H NMR. In an NMR tube charged with [RuH(NBD)(PCP)] (20 mg, 0.030 mmol), CD₃CN (0.05 mL), and CD₂Cl₂ (0.5 mL) was added DOTf (5 μL, 0.06 mmol) through a microsyringe. The mixture was allowed to stand for 30 min, and then NMR spectra were collected. The NMR spectra show that [Ru(CD₃CN)(NBD)(PCP)]OTf (**7d₃**), [Ru(CD₃CN)₃(PCP)]OTf (**8d₃**), and NBE are formed in a ratio of 3:2:2. NMR signals of **7d₃** are as follows. ³¹P{¹H} NMR (121.49 MHz, CD₂Cl₂): δ 54.5 (s). ¹H NMR (300.13 MHz, CD₂Cl₂): δ 0.76 (d, *J*(HH) = 8.9 Hz, 1H, C/H), 0.96 (d, *J*(HH) = 8.9 Hz, 1H, CH/H), 2.63 (s, 2H, CH), 3.09 (s, 2H, =CH), 4.14 (m, 2H, CH₂P), 4.55 (m, 2H, CH₂P), 5.23 (s, 2H, =CH), 7.03–8.01 (m, Ph, mixed with those of **8d₃**). NMR signals of **8d₃** are as follows. ³¹P{¹H} NMR (121.49 MHz, CD₂Cl₂): δ 49.5 (s). ¹H NMR (300.13 MHz, CD₂Cl₂): δ 3.94 (t, 4H, *J*(PH) = 3.9 Hz, CH₂P), 7.03–8.01 (m, Ph, mixed with those of **7d₃**). NMR signals of NBE are as follows. ¹H NMR (300.13 MHz, CD₂Cl₂): δ 1.00 (br, 2H, endo-CH₂), 1.15 (br, 1H, CH₂), 1.35 (br, 1H, CH₂), 1.69 (br, 2H, exo-CH₂), 2.93 (s, 2H, bridgehead CH), 6.03 (s, 2H, =CH).

Protonation of [RuH(NBD)(PCP)] with HOTf in the Presence of CH₃CN in CH₂Cl₂ and Identification of complexes **7 and **8** by NMR.** In an NMR tube charged with [RuH(NBD)(PCP)] (20 mg, 0.030 mmol), CH₃CN (0.05 mL), and CH₂Cl₂ (0.5 mL) was added HOTf (5 μL, 0.06 mmol) through a microsyringe. The mixture was allowed to stand for 30 min. The volatile materials were removed under vacuum. To the residue was added CD₂Cl₂ (0.5 mL), and then NMR spectra were collected. The NMR spectra show that [Ru(CH₃CN)(PCP)(NBD)]OTf (**7**) and [Ru(CH₃CN)₃(PCP)]OTf (**8**) are present in a ratio of 3/2. NMR signals of **7** are as follows. ³¹P{¹H} NMR (121.49 MHz, CD₂Cl₂): δ 54.5 (s). ¹H NMR (300.13 MHz, CD₂Cl₂): δ 0.78 (d, *J*(HH) = 8.9 Hz, 1H, C/H), 0.99 (d, *J*(HH) = 8.9 Hz, 1H, CH/H), 1.42 (s, 3H, CH₃CN, mixed with those of **8**), 2.64 (s, 2H, CH), 3.11 (s, 2H, =CH), 4.16 (m, 2H, CH₂P), 4.57 (m, 2H, CH₂P), 5.25 (s, 2H, =CH), 7.20–8.02 (m, Ph, mixed with those of **8**). NMR signals of **8** are as follows. ³¹P{¹H} NMR (121.49 MHz, CD₂Cl₂): δ 49.5 (s, [Ru(CH₃CN)₃(PCP)]OTf). ¹H NMR (300.13 MHz, CD₂Cl₂): δ 1.42 (s, 9H, CH₃CN, mixed with those of **7**), 3.98 (t, 4H, *J*(PH) = 3.9 Hz, CH₂P), 7.20–8.02 (m, Ph, mixed with those of **7**).

Protonation of [RuH(NBD)(PCP)] with DOTf in the Presence of CH₃CN in CH₂Cl₂ and Identification of Deuterated NBE by ²H NMR. To an NMR tube charged with [RuH(NBD)(PCP)] (20 mg, 0.030 mmol), CH₃CN (0.05 mL), and CH₂Cl₂ (0.7 mL) was added DOTf (5 μL, 0.06 mmol) through a microsyringe. The mixture was allowed to stand for 1 h. After the solution was treated with NaOH, the volatile portion was separated by vacuum transfer. The ²H NMR (61.25 MHz, CH₂Cl₂) of the resulting solution showed a singlet at 0.95 ppm.

Crystallographic Analysis. Crystals suitable for X-ray diffraction were grown from CH₂Cl₂ solutions of [RuCl(NBD)(PCP)] (**2**), [Ru(OAc)(PPh₃)(PCP)] (**6**), and [Ru(MeCN)(NBD)(PCP)]OTf (**7**) layered with hexane. All of the intensity data were collected on a Bruker SMART CCD area detector with graphite-monochromated Mo K α radiation at room temperature and corrected for absorption by SADABS (Siemens Area Detector Absorption).³³ All structures were solved by direct methods, expanded by difference Fourier syntheses, and refined by full-matrix least squares on *F*² using the Bruker SHELXTL (version 5.10)³⁴ program package. All non-hydrogen

(33) Sheldrick, G. M. SADABS, Empirical Absorption Correction Program; University of Göttingen, Göttingen, Germany, 1996.

atoms were refined anisotropically. Hydrogen atoms were placed in ideal positions and refined as riding atoms, except those for the acetonitrile ligand in **7**, which were located from the difference Fourier map and constrained to ride on the respective carbon (C62). In the case of **7**, after initial full-matrix least-squares refinement, the OTf anion exhibited distorted CF₃ and SO₃ groups, due to the large thermal motion of the terminal O and F atoms, and was subjected to fixed C–F and S–O distance restraints in the further refinement. Further crystallographic details are summarized in Table 1.

Computational Details. In the calculations, the phenyl groups of the PCP ligand have been modeled using hydrogen atoms. Geometry optimizations and frequency calculations have been performed for all species (reactants, intermediates, transition states, and products) involved in the reaction. All calculations have been carried out at the B3LYP level of density functional theory.³⁵ The LANL2DZ effective core potentials and basis sets³⁶ were used to describe the Ru and P atoms, while the standard 6-31G basis set³⁷ was used for C and H atoms. Polarization functions were added for hydrogen ($\xi(p) = 1.1$)³⁸ involved in the transfer processes. Transition states are confirmed by frequency calculations with the same density functional theory, effective core potentials, and basis

sets. All calculations were performed using the Gaussian 98 program³⁹ installed on Pentium III/IV personal computers with Linux (Red Hat) operating systems.

Acknowledgment. We acknowledge financial support from the Hong Kong Research Grants Council.

Supporting Information Available: Tables of crystallographic details, bond distances and angles, atomic coordinates and equivalent isotropic displacement coefficients, and anisotropic displacement coefficients for [RuCl(NBD)(PCP)] (**2**), [Ru(OAc)(PPh₃)(PCP)] (**6**), and [Ru(MeCN)(NBD)(PCP)]OTf (**7**); data are also available as files in CIF format. This material is available free of charge via the Internet at <http://pubs.acs.org>.

OM020521Q

(38) Andzelm, J.; Huzinaga, S. *Gaussian Basis Sets for Molecular Calculations*; Elsevier: New York, 1984.

(39) Frisch, M. J.; Trucks, G. W.; Schlegel, H. B.; Scuseria, G. E.; Robb, M. A.; Cheeseman, J. R.; Zakrzewski, V. G.; Montgomery, J. A., Jr.; Stratmann, R. E.; Burant, J. C.; Dapprich, S.; Millam, J. M.; Daniels, A. D.; Kudin, K. N.; Strain, M. C.; Farkas, O.; Tomasi, J.; Barone, V.; Cossi, M.; Cammi, R.; Mennucci, B.; Pomelli, C.; Adamo, C.; Clifford, S.; Ochterski, J.; Petersson, G. A.; Ayala, P. Y.; Cui, Q.; Morokuma, K.; Malick, D. K.; Rabuck, A. D.; Raghavachari, K.; Foresman, J. B.; Cioslowski, J.; Ortiz, J. V.; Stefanov, B. B.; Liu, G.; Liashenko, A.; Piskorz, P.; Komaromi, I.; Gomperts, R.; Martin, R. L.; Fox, D. J.; Keith, T.; Al-Laham, M. A.; Peng, C. Y.; Nanayakkara, A.; Gonzalez, C.; Challacombe, M.; Gill, P. M. W.; Johnson, B. G.; Chen, W.; Wong, M. W.; Andres, J. L.; Head-Gordon, M.; Replogle, E. S.; Pople, J. A. *Gaussian 98*, revision A.5; Gaussian, Inc.: Pittsburgh, PA, 1998.

(34) *SHELXTL Reference Manual (version 5.1)*; Bruker Analytical X-ray Systems: Madison, WI, 1997.

(35) (a) Becke, A. D. *Phys. Rev. A* **1988**, *38*, 3098. (b) Miehlich, B.; Savin, A.; Stoll, H.; Preuss, H. *Chem. Phys. Lett.* **1989**, *157*, 200. (c) Lee, C.; Yang, W.; Parr, G. *Phys. Rev. B* **1988**, *37*, 785.

(36) Hay, P. J.; Wadt, W. R. *J. Chem. Phys.* **1995**, *82*, 299.

(37) (a) Gordon, M. S. *Chem. Phys. Lett.* **1980**, *76*, 163. (b) Hariharan, P. C.; Pople, J. A. *Theor. Chim. Acta* **1973**, *28*, 213. (c) Binning, R. C., Jr.; Curtiss, L. A. *J. Comput. Chem.* **1990**, *11*, 1206.